








**Please cite the Published Version**

Apeh, Victor Onukwube , Okafor, Kennedy Chinedu , Chukwuma, Ifeoma Felicia , Uzoeto, Henrietta Onyinye , Chinebu, Titus Ifeanyi , Nworah, Florence Nkechi , Edache, Emmanuel Israel, Okafor, Ijeoma Peace and Anthony, Okoronkwo Chukwunenye  (2024) Exploring the potential of aqueous extracts of *Artemisia annua* ANAMED (A3) for developing new antimalarial agents: In vivo and silico computational approach. *Engineering Reports*, 6 (9). e12831 ISSN 2577-8196

**DOI:** <https://doi.org/10.1002/eng2.12831>

**Publisher:** Wiley

**Version:** Published Version

**Downloaded from:** <https://e-space.mmu.ac.uk/635666/>

**Usage rights:**  [Creative Commons: Attribution 4.0](https://creativecommons.org/licenses/by/4.0/)







**Additional Information:** This is an open access article published in *Engineering Reports*, by Wiley.

**Data Access Statement:** The current work created or examined data sets, which will be made available upon justifiable request.

**Enquiries:**

If you have questions about this document, contact [openresearch@mmu.ac.uk](mailto:openresearch@mmu.ac.uk). Please include the URL of the record in e-space. If you believe that your, or a third party's rights have been compromised through this document please see our Take Down policy (available from <https://www.mmu.ac.uk/library/using-the-library/policies-and-guidelines>)

# Exploring the potential of aqueous extracts of *Artemisia annua* ANAMED (A3) for developing new anti-malarial agents: In vivo and silico computational approach

Victor Onukwube Apeh<sup>1</sup>  | Kennedy Chinedu Okafor<sup>2,3</sup>  |  
 Ifeoma Felicia Chukwuma<sup>4</sup>  | Henrietta Onyinye Uzoeto<sup>1</sup>  |  
 Titus Ifeanyi Chinebu<sup>1</sup>  | Florence Nkechi Nworah<sup>4</sup>  | Emmanuel Israel Edache<sup>5</sup> |  
 Ijeoma Peace Okafor<sup>6</sup> | Okoronkwo Chukwunenye Anthony<sup>3</sup> 

<sup>1</sup>Federal College of Dental Technology and Therapy, Enugu, Department of Applied Sciences, Enugu, Nigeria

<sup>2</sup>Department of Engineering, Faculty of Science and Engineering, Manchester Metropolitan University, Manchester, UK

<sup>3</sup>Department of Mechatronics Engineering, School of Electrical Systems Engineering and Technology (SESET), Federal University of Technology, Owerri, Nigeria

<sup>4</sup>Department of Biochemistry, Faculty of Biological Sciences, Nsukka, Nigeria

<sup>5</sup>Department of Pure and Applied Chemistry, University of Maiduguri, Maiduguri, Nigeria

<sup>6</sup>Department of Applied Public Health, Cardiff Metropolitan University, Cardiff, UK

## Correspondence

Kennedy Chinedu Okafor, Manchester Metropolitan University, Department of Engineering, All Saints, Manchester M15 6BH, Manchester, UK M1 5GD, UK.  
 Email: [k.okafor@mmu.ac.uk](mailto:k.okafor@mmu.ac.uk)

## Funding information

Tertiary Education Fund, Grant/Award Number: TETF/ES/UNIV/IMO STATE/TSAS/2021

## Abstract

The emergence of resistance to current antimalarial drugs poses a significant challenge in the fight against malaria. This study aimed to investigate the in vivo antiplasmodial potential of the aqueous extract of fresh and dried leaves of A3 in *Plasmodium berghei*-infected (*P. berghei*) mice. A 4-day suppressive test was conducted, with infected BALB/c mice receiving artesunate and A3 extracts. The results showed that the tested doses of A3 attenuated the elevation of parasitemia induced by *P. berghei*, particularly at the dose of 400 mg/kg, and improved hematological indices. Computational techniques, including molecular docking, binding free energy calculations, and ADMET predictions, identified several bioactive compounds in A3 with promising inhibitory potential against lysyl-tRNA synthetases and Dihydrofolate reductase (DHFR), the crucial enzymes targeted by antimalarial drugs. In this paper, Friedelin, Bauerenol, Epifriedelanol, Alpha-Amyrenone, Stigmasterol, and beta-Amyrin acetate were top-ranked, having docking scores from  $-10.6$  to  $-9.9$  kcal/mol, compared with the  $-9.4$  and  $-7.1$  kcal/mol demonstrated by artesunate and chloroquine, respectively, as standard ligands. Also, it was shown that docking score from the Lysyl-tRNA protein target (4YCV) ranged from  $-9.5$  to  $-7.8$  kcal/mol in comparison to artesunate (8.1 kcal/mol) and chloroquine (5.6 kcal/mol). The results suggest that the identified compounds in A3 could serve as potential candidates for the development of new anti-malarial agents.

## KEYWORDS

ANAMED, *Artemisia annua*, bioengineering, computational biology, computational techniques, disease predictions, molecular docking

This is an open access article under the terms of the [Creative Commons Attribution](https://creativecommons.org/licenses/by/4.0/) License, which permits use, distribution and reproduction in any medium, provided the original work is properly cited.

© 2023 The Authors. *Engineering Reports* published by John Wiley & Sons Ltd.

## 1 | INTRODUCTION

Malaria is a severe public health concern, particularly in sub-Saharan Africa and other subtropical regions. In 2020, there were approximately 241 million malaria cases, with *Plasmodium falciparum* and *Plasmodium vivax* being the main culprits for deaths, especially in children under five and pregnant women. The spread of resistance to Artemisinin-based Combination Therapy (ACT) by these parasites poses a significant threat to malaria chemotherapy.<sup>1</sup> Concerns have been raised about the loss of the only highly effective treatment available. Molecular markers of artemisinin resistance have been identified, and research is focusing on the identification of inhibitors for crucial enzymes like dihydrofolate reductase and lysyl-tRNA synthetase.

Medicinal plants, such as *Artemisia annua*, have shown promise as sources of antimalarial and antimicrobial compounds (Manesh et al., 2023).<sup>2</sup> The A3 strain of *Artemisia annua*, with its unique properties, has exhibited positive effects against resistant malaria symptoms and the potential for treating other diseases. Extracts from A3 have shown inhibition of plasmodia enzymes, but it is unclear which extracts provide plasmodia clearance.

Malaria relapse after treatment has been largely linked to antimalarial resistance; this has generated disquiet among clinicians. The paper,<sup>3</sup> discussed the mode of action of Artemisinin and emphasized the potent antimalarial properties of the amino-artemisinin derivatives Artemisone and artemiside. Unlike artemisinins, which are believed to act through peroxide group activation, these derivatives exhibited distinct effects on the apicomplexan parasite *T. gondii*. Resistance to Artemisone and artemiside in *T. gondii* strains was observed, revealing downregulation of specific proteins, especially those associated with ROS scavenging. The authors<sup>4</sup> examined the essential function of artemisinin in antimalarial therapy along with its historical history, present applications, and the burgeoning problem of *Plasmodium falciparum* resistance. A notable major observation is that the spread of the parasites with decreased sensitivity threatens malaria control efforts. Molecular markers of artemisinin resistance have been validated through several mutations.<sup>5</sup> Since dihydrofolate reductase and lysyl-tRNA synthetase are crucial for the growth of parasites, research is increasingly concentrating on the identification of these enzymes' inhibitors. From a medicinal chemistry standpoint, DHFR is of great importance due to its role in cell proliferation, purine, and thymidylate production, and folate metabolism.<sup>6</sup> In the last decade, *Plasmodium* aminoacyl-tRNA synthetases have drawn more attention as potential novel targets for the development of antimalarial drugs.<sup>7</sup> Lysyl-transfer RNA, or Lys-tRNA (Lys), is created through the action of the enzyme lysyl-tRNA synthetase and is subsequently prepared to add lysine to proteins. Hence, Lysyl-tRNA synthetase targeting is still required to test novel chemical scaffolds with improved antimalarial effectiveness.<sup>8</sup> Medicinal plants may be a source of chemicals with powerful antimalarial and antimicrobial properties.<sup>9</sup>

The *Artemisia annua* of ANAMED (Action for Natural Medicine) fondly known as A<sup>3</sup> is a hybrid plant of *Artemisia annua* with unique antimalarial, antibacterial, and antifungal potentials. The new strain—A3—adapted to tropical conditions has been introduced to Upper Room Ministries Ugwuomu-Nike in southeastern Nigeria for cultivation according to the guidelines ANAMED. It has been proven to exhibit positive effects against resistant malaria symptoms and exhibits potential for other diseases such as dysmehnorria, and asthma to mention but a few. Several reports in the References 10-12 have suggested that artemisia, its components, and/or artemisinin derivatives help prevent plasmodia infection by reducing oxidative stress related to the mechanism of action of malaria chemotherapy and preventing invasion and inflammation. Artemisinin and its derivatives have also had a significant impact on the development of malaria chemotherapy.<sup>2</sup> The World Health Organization (WHO) recommends ACTs.<sup>13</sup> Tea therapy is also available and has proven to be effective against all forms of malaria partly due to the input of another bioactive compound, which is favored by low-income populations for its affordability. A<sup>3</sup> extracts have demonstrated inhibition of plasmodia enzymes but it is not known which of the extracts provides plasmodia clearance.

A recent investigation by Zhou et al.<sup>14</sup> showed that *Artemisa annua* hot-water extract demonstrated its capability of inhibiting SARS-COV-2 spike glycoprotein and its variants. It has also been reported to control the proliferation of pro-inflammatory cytokines and stimulate reactive oxygen species generation.<sup>15</sup> It has been suggested by du Preez-Bruwer et al.<sup>16</sup> that the antimalarial activity of *Artemisia annua* could be linked to a possible synergy between other *Artemisa annua* compounds and artemisinin. However, there have been reports of antimalarial characteristics of other plants,<sup>17-19</sup> but the impact of solvent extraction on the percentage of parasitaemia clearance has received little consideration. With the current threat of drug resistance and other untoward effects, the focus of the study is to assess the in silico and ADMET properties of the isolated A3 compounds, as well as the antimalarial potentials of the extracts using computational experimentations.

## 1.1 | Problem statement and contributions

Given the ongoing global health challenge posed by malaria, affecting millions annually, the rise of drug-resistant malaria parasite strains has significantly complicated treatment and control strategies. In recent years, there has been a rise in interest as regards leveraging computational biology methodologies to explore the antimalarial properties encoded in the genomes of medicinal plants. Traditional medicine has historically recognized the therapeutic potential of various plant extracts, hinting at the prospect of uncovering bioactive compounds with antimalarial properties through computational analyses.

However, the existing research on the efficacy and safety of these medicinal plants is insufficient. This emphasizes the necessity for rigorous experimental investigations to decipher their antimalarial capabilities. Thus, there exists an urgent need to identify new therapeutic targets and advance the computational design and screening of innovative antimalarial drugs. One promising approach involves employing computational biology techniques to target essential enzymes crucial for the survival and replication of the malaria parasite. Two such enzymes namely: dihydrofolate reductase (DHFR) and lysyl-tRNA synthetase (LysRS), have been identified as computationally validated targets for malaria chemotherapy. DHFR computationally governs folate synthesis—an indispensable nutrient for the parasite—while LysRS is integral to protein synthesis. Computational biology approaches play a pivotal role in elucidating the effectiveness and safety profiles of potential antimalarial agents derived from medicinal plants and in validating the viability of computationally designed interventions targeting enzymes like DHFR and LysRS.

This study aims to address the following research questions:

- i. What are the specific compounds or extracts from medicinal plants that exhibit inhibitory effects on enzymes such as DHFR and LysRS?
- ii. How effective are these compounds or extracts in inhibiting the growth and replication of the malaria parasite?
- iii. Are there any potential side effects or toxicities associated with the use of these compounds or extracts?
- iv. Can these compounds or extracts be further developed into safe and effective antimalarial drugs?

By answering these research questions, this study aims to contribute to the development of new antimalarial strategies and provide valuable insights into the potential of medicinal plants as a source of antimalarial compounds. The findings may pave the way for the discovery of novel drugs that can effectively combat drug-resistant strains of malaria, ultimately improving the lives of millions affected by this debilitating disease.

## 2 | MATERIALS AND COMPUTATIONAL METHODS

### 2.1 | Materials collection

Fresh leaves of *Artemisia annua* L. (*A. annua*) were collected in August 2020 from Upper Room Ministry, Emene, Enugu East LGA of Enugu State, Nigeria, during the rainy season. The collected leaves were authenticated, and a voucher sample was placed at the University of Nigeria, Nsukka's (UNN) Department of Plant Sciences and Biotechnology Herbarium. The fronds were ground using an electric blender (Marlex Electrolyne IS: 250) after 3 weeks of air-drying. Each of the fresh and dry leaves, weighing 2000 g, was extracted using warm water (40°C). The macerates were left to stand for 72 h and periodically shaken for 20 min. These were then sieved using a muslin cloth and filtered with Whatman filter paper (No. 1). To produce a two-dry powder extract, the extracts were lyophilized. Before usage, the extracts were sterilized through a 0.22 µm membrane filter and reconstituted in 10% v/v tween 20.

### 2.2 | Phytochemical determination

Quantitative analysis of phytochemicals in AD and AF was performed under the procedure outlined by Nbaeyi-Nwaoha and Onwuka.<sup>20</sup> The process was repeated three times, and the results were computed using Equation (1).

$$\text{Phyd} = \frac{\text{Absorbance of Test}}{\text{Absorbance of Standard}} \times 100 \quad (1)$$

- **Alkaloids** : The pulverized samples of fresh and dry extracts, each weighing 1 g, were dissolved in 20 mL of 20% H<sub>2</sub>SO<sub>4</sub> in 1:1 ethanol before being filtered. Then 5 mL of 40% H<sub>2</sub>SO<sub>4</sub> were added and properly mixed after 1 mL of each of the filtrates (fresh and dry) had been added to two different test tubes. Before collecting the measurement, the mixture was covered and given 4 h to settle. A set of reference standard solutions of atropine (20, 40, 60, 80, and 100 µg/mL) were prepared in the same manner as described already. The absorbance for standard solutions and solutions was determined on the reagent blank at 568 nm wavelength with a spectrophotometer.
- **Tannins** : One gram of ground fresh and dry *A. annua* leaves from separate conical flasks were mixed with 10 mL of water, shaken for 30 min at intervals of 5 min, and then filtered. Two separate conical flasks were filled with a constant amount (2.5 mL) of each filtrate, 1 mL of Follin-Denis reagent, and 1 mL of Na<sub>2</sub>CO<sub>3</sub>, and everything was thoroughly mixed. A set of standard solutions of gallic acid (20, 40, 60, 80, and 100 µg/mL) were prepared as described earlier; the combination was left to stay for 90 min at room temperature before the absorbance at 720 nm was measured.
- **Saponins** : In separate conical flasks, 1 g of the ground samples of fresh and dried *A. annua* leaves and 0.2500 g of tea saponin standard were mixed with 10 mL of petroleum ether. Ten milliliters of petroleum ether was added to it after further mixing, and it was then washed and dried. Following thorough mixing of the dry mixture with ethanol (5 mL), each sample received around 2 mL of the mixture, which was then placed in one of the two test tubes and left to settle for 30 min. Absorbance of standard and test solutions was analyzed with blank at 550 nm wavelength.
- **Flavonoids** : The pulverized samples of fresh and dry *A. annua*, weighing 1 g each, were dissolved in 200 mL of ethyl and then filtered. Two distinct test tubes were filled with 5 mL of fresh and dry filtrates each. Five milliliters of diluted ammonia was then added, forcefully mixed, and left to sit for a few hours. Standard solutions of quercetin (20, 40, 60, 80, and 100 µg/mL) were prepared as expressed earlier. The absorbance was measured for test and standard solutions using a reagent blank at 490 nm wavelength.

### 2.3 | Determination of mineral compositions (fresh and dry leaf samples of A<sup>3</sup>)

The presence of the following minerals—Zinc (Zn), Iron (Fe), and Selenium (Se), contents of each sample were determined by the atomic absorption spectrophotometer (AAS). After being assayed in a muffle furnace at 550°, each sample (2 g) was examined for minerals using a Mode 303 Perkin-Elmer spectrophotometer for atomic absorption (AAS) at Norwalk, USA.

### 2.4 | Determination of vitamin contents (fresh and dry A3)

The high-performance liquid chromatography (HPLC) method was used to quantify vitamins using diode array (DAD) and light scattering (LDD) detectors along with PERKIN ELMER® HPLC equipment. The following chromatographic parameters were used: oven temperature of 30°C, flow rate of 1.0 mL/min, injection volume of 100 L, detection wavelengths of 210 nm (B6), 283 nm (B6, B9, B12, C), 361 nm (B12), 325 (A), and 265 (D3). Three duplicates of each measurement were made. For water-soluble vitamins (B12, and C), one chromatographic technique was used, and the other was for fat-soluble vitamins (E). While the second one contained an acetonitrile ramp and 25 mM phosphate buffer, pH 3.32, the first one employed an isocratic technique (99% methanol: HPLC water).

### 2.5 | Case study

#### 2.5.1 | Ethical considerations

Approval for the handling of the animals was granted under reference number (AREC/PS/22/714) by the Ethical Committee on the Use and Care of Experimental Animals at the Faculty of Pharmaceutical Sciences, University of Nigeria, Nsukka. The animals were treated following the committee's guidelines.



## 2.5.2 | In vivo setup

In this section, animal context will be discussed. The Faculty of Pharmaceutical Sciences, University of Nigeria, Nsukka (UNN) provided the Swiss albino mice used in this experiment. These were 10–12 weeks old and weighed 2–2.8 g. During their 7-day adjustment period, food was given regularly as well as water at will. The mice were housed at the Animal Housing Unit of the Faculty of Pharmaceutical Sciences, UNN.

## 2.5.3 | Determination of extract toxicity

Using the Lorke<sup>21</sup> approach, the median lethal dosage (LD<sub>50</sub>) was computed to determine the extract's acute toxicity. The procedure involved giving the six groups of Swiss albino mice various doses of *Artemisia annua*—10, 100, 1000, 1600, 2900, and 5000 mg/kg. Following that, the occurrence of physical symptoms in mice and mortality were observed for potential harm.

## 2.5.4 | Parasites

The parasite used is *Plasmodium berghei* NK 65, a mouse-bred, chloroquine-sensitive strain from the Parasitology Division of the Department of Zoology UNN. This parasite was then transferred into new mice used in this investigation as donor mice.

## 2.5.5 | In vivo schizonticidal activity

This was done under protocol after Peter's 4-day suppression test.<sup>22</sup> The donor mice's % parasitaemia and red blood cell count were measured on Day 0 of this test using a Giemsa-stained thin blood smear and an upgraded Neubauer Counting Chamber. The blood was then diluted with physiological saline (normal saline) to give a concentration of  $10^8$  parasitized erythrocytes per ml after being drawn from the retro-orbital plexus vein of the donor mice. Each of the experimental mice received an intraperitoneal injection of  $2 \times 10^7$  parasitized erythrocytes (0.2 mL of  $10^8$  parasitized erythrocytes/mL). All the animals utilized were infected from the same source to avoid variation in parasitaemia.

There were seven groups of mice, each with five animals, at random. Four hours after the infection, the first course of treatment commenced. One group got 5 mg/kg artesunate per day (standard control), while two groups (baseline and untreated groups) received normal saline. Two of the groups were given 200 and another two groups received 400 mg/kg of the A<sup>3</sup> extract of aqueous solvents (fresh and dry) per day, orally. At 4, 24, 48, and 72 h after infection, the same quantities of the standard drug, extract, and normal saline were received. Individual radio frequency identification-tagged mice in cages were monitored using an automatic feeder that also measured their body weight and physical characteristics. Here, we show that this tracking device can identify symptoms of illness (such as loss of appetite) within 2–4 h after a *Plasmodium berghei* infection, where human inspectors performing routine health checks are unable to track down a notable difference between infected groups and baseline. The animals received a sufficient diet, and no deaths were noted during the experiment.

## 2.6 | Parasitaemia level measurement

Using properly labeled and clean slides, thin blood films were produced on test day 4.<sup>23</sup> Blood was taken from the retro-orbital plexus vein of each animal using a heparinized capillary tube. After being fixed with methanol, the dried blood films were stained with Giemsa and allowed to stand for 25 min. Following a phosphate buffer wash with a pH of 7.2, they were left to dry.<sup>24</sup> To guarantee the best possible film quality control, a total of 70 slides, one for each animal, were produced. The slides were viewed under a model Olympus microscope at  $\times 100$  magnification while submerged in oil.<sup>24</sup> The percentage suppression of parasitaemia at each dose level was calculated by contrasting the levels of parasitaemia

in infected and uninfected controls. The average percentage suppression of parasitaemia was calculated using the formula: where  $A$  is the Average percentage suppression.  $B$  is the Average percentage parasitaemia in the placebo group.  $C$  is the Average percentage parasitaemia in the test group.<sup>25</sup>

$$\text{Parasitemia (\%)} = \frac{\text{Number of parasitized red blood cell}(n-1)x^2}{\text{Number of total red blood cell count}} \times 100 \quad (2)$$

Finally, the Equation (3) was used to obtain the mean percentage of parasitemia suppression as:

$$\text{Suppression (\%)} = \frac{B-C}{B} \times 100 \quad (3)$$

After 4 days of treatment, the mice appeared extremely healthy and lively. After that, these were observed for 30 days. The treated mice were all conscious and moving around. Unfortunately, 10 days following the trial, two of the untreated mice passed away.

## 2.7 | Full blood count assays

According to Apeh et al.,<sup>26</sup> full blood counts were calculated using the Sysmex® Automated Hematology Analyzer KX-21 N, made by Sysmex Corporation in Kobe, Japan. These counts included PCV, Hb, RBC, WBC, differential WBC (lymphocytes and mixed), and red cell indices (MCHC, MCH, and MCV).

## 2.8 | In silico research

### 2.8.1 | Preparation of protein for docking

The two anti-malaria enzymes' 3D crystalline structures and a crystallographic resolution were retrieved from the Protein Data Bank (PDB) ([www.rcsb.org](http://www.rcsb.org)) repository as follows: 2BL9 is 1.9 Å while 4YCV is 3.41 Å. The protein was viewed with the Discovery studio visualizer. Polar hydrogen was added after water molecules were taken away from the protein. The protein's active site and the grid map were generated with AutoDockFR as reported by Ravindranath et al.<sup>27</sup> The used grid center ( $x$ ,  $y$ , and  $z$ ) and receptors are as follows: 2BL9 (83.1223, 9.9806, 31.6705) and 4YCV (18.9975, -1.0113, 62.9525), respectively.

### 2.8.2 | Ligand library propagation

The SDF format was used to download compounds (168) from Dr. Duke's Phytochemical and Ethnobotanical database (U.S. Department of Agriculture, Agricultural Research Service).<sup>28</sup> Using the universal force field (UFF) and steepest descent technique, Avogadro v1.2 software was used to pre-optimize the 3D structures of the phytochemical compounds and subsequently optimized using MOPAC v22.0.4 software with semi-empirical PM7 method.<sup>29</sup> The optimized chemical structures were saved in a PDF file using the Avogadro software.

### 2.8.3 | Molecular docking

The protein and ligand structures were transformed using PyRx v0.8 software<sup>30</sup> from .pdb to .pdbqt file for molecular docking. Multiple docking approach was employed between the phytochemical compounds against the 3D protein structures using PyRx v0.8 virtual screening tool with AutoDock-vina wizard.<sup>31</sup> The Discovery studio's visualizer was used to view the 2D and 3D interactions of the best ligands. The selected ligands after the blind docking are: Friedelin, Bauerenol, Epifriedelanol, Alpha-Amyrenone, Stigmasterol, Beta-Amyrin acetate, Cynaroside, Quercimeritrin, Chrysoeriol, Luteolin, Isorhamnetin and Quercetin while the standard ligands used were artesunate and chloroquine.

## 2.8.4 | ADME analysis of top selected compounds

To be considered orally ingested medications, drug candidates must first satisfy several requirements as a fundamental step of the drug discovery process. Drug similarity attributes Lipinski et al. rule, physicochemical properties (molecular weight, H bonding, heavy atoms, etc.), bioavailability, water solubility, pharmacokinetics, and stability were assessed.<sup>32</sup> Using the SwissADME website (<http://www.swissadme.ch/>), the ADMET properties of the most highly ranked compounds were investigated in this study.

## 2.9 | Statistical analysis

In this paper, Graph Pad Prism version 6.05 one-way ANOVA and Turkey's post hoc multiple comparisons were used to analyze the raw data set. In Section 3, \* $p < 0.05$ , \*\* $p < 0.01$ , or \*\*\* $p < 0.001$  was used to indicate significance in the data which is presented as mean  $\pm$  SDs (SD) in Section 3.

## 3 | RESULTS

### 3.1 | Phytochemical constituents of *Artemisia annua* ANAMED

Table 1 shows the phytochemical composition of different extracts of *Artemisia annua*. It was observed that saponin was significantly higher ( $p < 0.05$ ) in dry leaf extract (AD) when compared with fresh leaf extract (AF). Also, significantly higher ( $p < 0.05$ ) values of flavonoids, alkaloids, and tannins in AD were recorded when compared with the AF counterparts. The examination of phytochemical concentrations yielded the following decreasing order of phytochemical concentrations: Saponin > flavonoids > alkaloids > tannins in both AD and AF.

### 3.2 | Mineral compositions of *Artemisia annua* ANAMED (A3) leaf extract

Table 2 shows the mineral composition of A3 leaf extracts. This revealed that it is very rich in iron and was significantly more ( $p < 0.05$ ) in AD than that in the AF counterparts. Interestingly, zinc and copper recorded higher concentrations in AD when compared with the AF; Copper, however, did not show a notable difference ( $p > 0.05$ ) in either AD or AF. Surprisingly there was no presence of selenium in both AF and AD.

**TABLE 1** Aqueous extract of fresh *Artemisia annua* (AF) and dry *Artemisia annua* (AD).

Phytochemicals (%)	Aqueous fresh	Aqueous dry
Alkaloids	2.080 $\pm$ 0.060a	2.680 $\pm$ 0.026b
Tannins	0.029 $\pm$ 0.002a	0.066 $\pm$ 0.005b
Saponin	2.777 $\pm$ 0.042a	3.967 $\pm$ 0.045b
Flavonoids	2.183 $\pm$ 0.015a	3.683 $\pm$ 0.040b

Note: Mean  $\pm$  SD of triplicate experiments. Means were compared using one-way ANOVA. In each row, values with different letters (superscript) indicate significant differences at  $p < 0.05$ . AD = Dry sample soaked in aqueous solution; AF = Fresh sample soaked in aqueous solution. These results are further discussed in Section 4.

**TABLE 2** Mineral compositions of fresh and dry leaf samples of A3.

Minerals (mg/100 g)	AF	AD
Fe (mg/100 g)	7.890 $\pm$ 0.020a	11.60 $\pm$ 0.139b
Zn (mg/100 g)	1.970 $\pm$ 0.020a	2.357 $\pm$ 0.035b
Se (mg/100 g)	0 $\pm$ 0	0 $\pm$ 0
Cu (mg/100 g)	0.038 $\pm$ 0.002a	0.039 $\pm$ 0.002a

Note: Mean  $\pm$  SD of triplicate experiments. Means were compared using one-way ANOVA. In each row, values with different letters (superscript) indicate significant differences at  $p < 0.05$ . AD = Dry sample soaked in aqueous solution; AF = Fresh sample soaked in aqueous solution.



### 3.3 | Vitamin composition of fresh and dry leaf of A3

Table 3 shows the Vitamin contents of Fresh and dry. The result expressed a remarkably rich content of vitamin C in both AD and AF; compared to AF, this was considerably higher in AD ( $p < 0.05$ ). Similarly, the vitamin E content of AD was significantly higher than the AF counterpart. Amazingly, there was no presence of vitamin B12 in both AD and AF.

### 3.4 | Median lethal dose and acute toxicity study (LD50) of aqueous A3

As shown in Table 4, there were no recorded mortalities among all experimental mice. The median lethal dose of the extracts of fresh and dry *Artemisia annua* ANAMED was shown to be above 5000 mg/kg by Lorke's method. No physical or behavioral signs suggest that the extract was nontoxic and safe for administration orally at the higher limit dose of 5000 mg/kg Body weight.

### 3.5 | Percentage of parasitaemia and suppression of Plasmodium beghei

The percentage parasitaemia and suppression of Plasmodium beghei as shown in Figure 1 revealed decreased parasitaemia under the concentration of the dose. Compared to the 200 mg/kg bw treated groups, there was a decrease in the 400 mg/kg bw treated groups. Similarly, it was also observed that there was increased antimalaria activity in aqueous dry extract (AD) when compared to the aqueous fresh extract (AF). In the same vein, the percentage suppression tests indicate that there was an increased suppression of parasitaemia in a dose-dependent pattern; with the 400 mg/kg bw treated group exhibiting a higher suppression when compared to the 200 mg/kg bw-treated group. There was a higher % of parasite suppression in 400 mg/kg bw of AD in comparison with artesunate-treated group suggesting a higher domiciliation of antimalaria potentials in AD.

### 3.6 | Hematological indices of parasitized mice treated with Artemisia annua

The hematological indices of parasitized mice treated with *Artemisia annua* ANAMED (A3), standard drugs, and untreated were evaluated ad shown in Figure 2. PCV and RBC of the untreated group were found to have decreased significantly ( $p < 0.05$ ) from baseline levels. However, as compared to the untreated group, an artesunate-treated group did

TABLE 3 Vitamin contents of fresh and dry *Artemisia annua* ANAMED.

Vitamins	AF	AD
B12 ( $\mu\text{g}/100\text{g}$ )	$0 \pm 0$	$0 \pm 0$
C ( $\text{mg}/100\text{g}$ )	$39.69 \pm 0.020\text{a}$	$42.943 \pm 0.601\text{b}$
E ( $\text{mg}/100\text{g}$ )	$1.330 \pm 0.017\text{a}$	$2.423 \pm 0.015\text{b}$

Note: Mean  $\pm$  SD of triplicate experiments. Means were compared using one-way ANOVA. In each row, values with different letters (superscript) indicate significant differences at  $p < 0.05$ . AD = Dry sample soaked in aqueous solution; AF = Fresh sample soaked in aqueous solution.

TABLE 4 Median lethal dose and acute toxicity study (LD50) of A3.

Phases	Doses (mg/kg)	No. of mortality AD A3	No. of mortality AF A3
Phase I	10	Nil	nil
	100	Nil	nil
	1000	Nil	nil
Phase II	1600	Nil	nil
	2900	Nil	nil
	5000	Nil	nil

Note:  $n = 3$ .

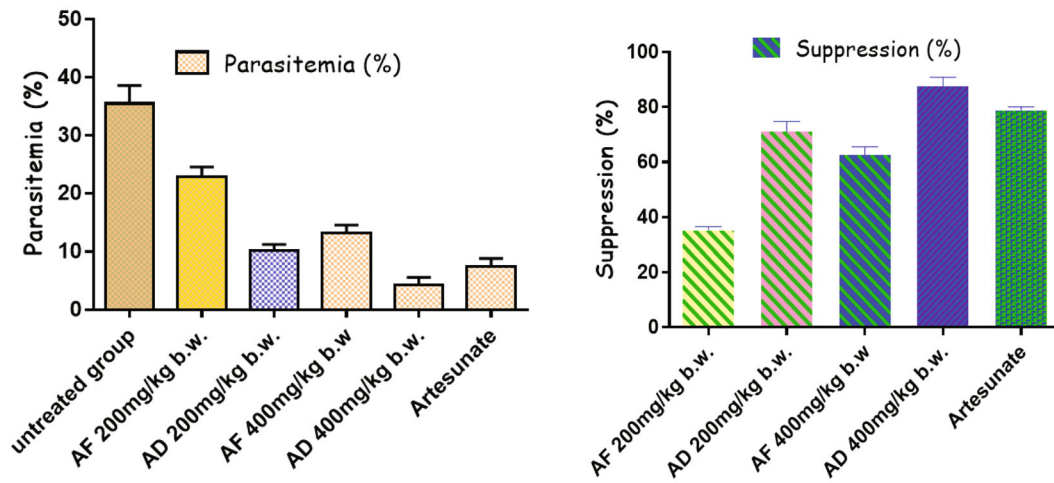


FIGURE 1 Percentage parasitaemia and suppression of the parasite after treatment.

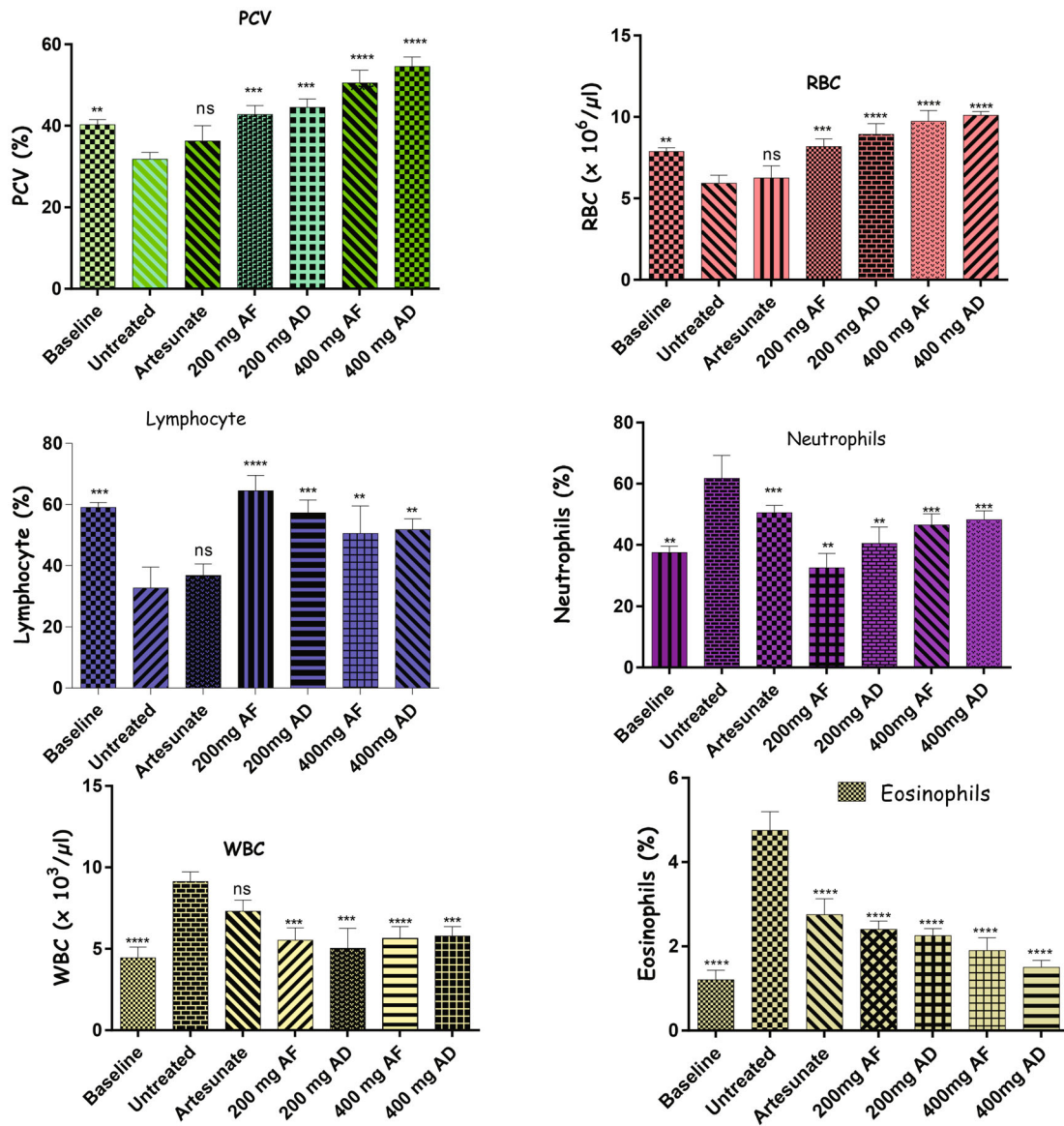


FIGURE 2 Effect of aqueous extract of A3 on hematological parameters of *Plasmodium berghei*—infected mice.

not show a significant rise ( $p > 0.05$ ); in contrast, artemisia-treated groups showed a significant increase. Additionally, there was no distinction between the artesunate-treated group and the control group ( $p > 0.05$ ), indicating that artesunate does not have any lymphocyte-inducing properties, while in neutrophil, compared to the untreated group, there was a statistically significant drop ( $p < 0.05$ ) in the artesunate-treated group. The 200 mg/kg bw treated group expressed the highest lymphocyte mobilization and lowest neutrophil mobilization in all the groups. As shown in Figure 2, total leucocytes indicate higher leucocyte mobilization in the untreated group; leucocytes in the artemisia-treated groups decreased significantly ( $p < 0.05$ ) as compared to the untreated group, suggesting that the infection is being resolved in those groups. Eosinophil, an index of parasitaemia, was highest in the untreated group. When compared to the untreated group, the treatment group saw a dose-dependent substantial decline during the same period. The hematological indices of extract-treated groups suggest an improvement of the differentials as well as the red cell indices when compared with the untreated.

### 3.7 | Molecular docking: Ligands from A3, and standard drugs

In this subsection, the molecular docking of ligands from A3, and standard drugs on target protein (2BL9) is investigated. From Table 5 and Figure 3B, the results of the molecular docking technique revealed that the

TABLE 5 Ligands interaction with dihydrofolate reductase (ID 2BL9) and its amino acid residues.

S/No.	Compound CID	Compound name	Molecular formula	Docking scores (kcal/mol)	Amino acid residues of 2BL9	Interaction types	Bond length (Å)
1	91,472	Friedelin	C30H50O	-10.6	PHE A 57	Pi-sigma	4.46
2	111,220	Baueranol	C30H50O	-10.5	PHE A: 57	Pi-Sigma/alkyl	4.36/6.92
					ILE A: 121	Pi-alkyl	5.44
3	119,242	Epifriedelanol	C30H52O	-10.3	PHE A: 57	Pi-sigma	4.40
					Val A: 204	Alkyl	6.59
4	12,306,155	Alpha-Amyrenone	C30H48O	-10.2	PHE A: 57 TYR A: 125	Pi-sigma	4.64
					MET A: 54	Pi-sigma	4.00
					TYR A: 179	Alkyl	5.92
					CYS A: 14	H-bond	6.47
5	5,280,794	Stigmasterol	C29H48O	-10.0	PHE A: 57	Pi-sigma/alkyl	4.22/4.92
					ILE A: 121	Pi-alkyl	7.49
					LEU A: 128	Alkyl	7.75
					LEU A: 45	Alkyl	5.23
6	92,156	Beta-Amyrin acetate	C32H52O2	-9.9	PHE A: 57	Pi-alkyl	6.68
7	6,917,864	Artesunate	C19H28O2	-9.4	PHE A: 57	Pi-alkyl	5.49
					ILE A: 121	Alkyl	6.94
					ALA A: 15	H-bond	3.60
					ILE A:173	H-bond	4.90
8	2719	Chloroquine	C18H26ClN3	-7.1	ILE A:173	H-bond	4.68
					ILE A: 121	Alkyl	4.74
					PHE A: 57	Pi-pi-stacked	5.28
					LEU A: 45	Alkyl	4.79
					ASP A:53	Carbon-H	5.80

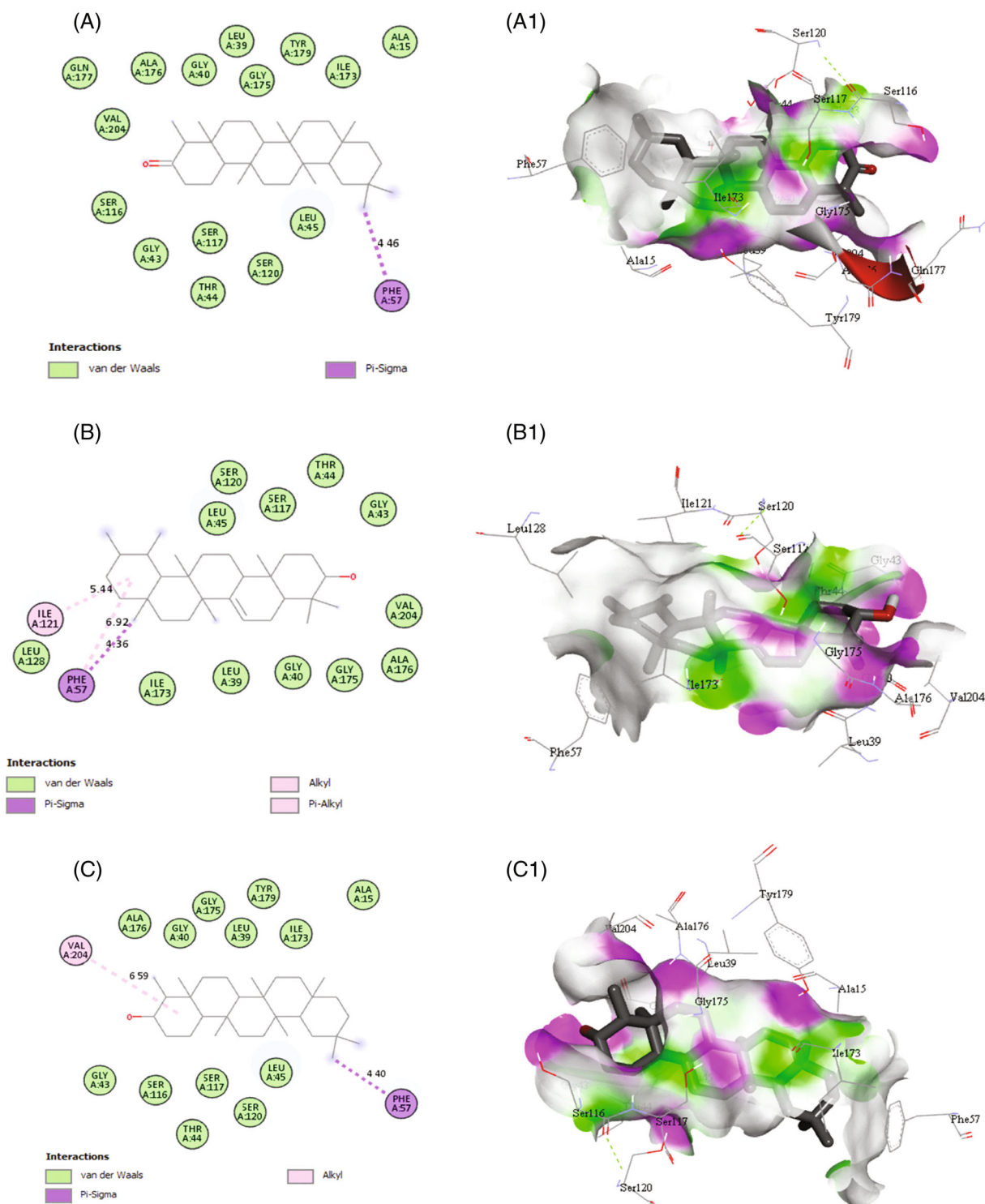


**FIGURE 3** 2D and 3D interaction of ligands and Amino acid residues of 2BL9. This shows individual interactions and key amino acid residues for the inhibitor binding between 2BL9 and (A): Friedelin, (B): Bauerenol, and (C): Epifriedelanol. A–C: 2D interactions, A1–C1: 3D interactions. (D): Alpha-Amyrenone, (E): Artesunate, and (F): Chloroquine. (D–F): 2D interactions, (D1–F1): 3D interactions.



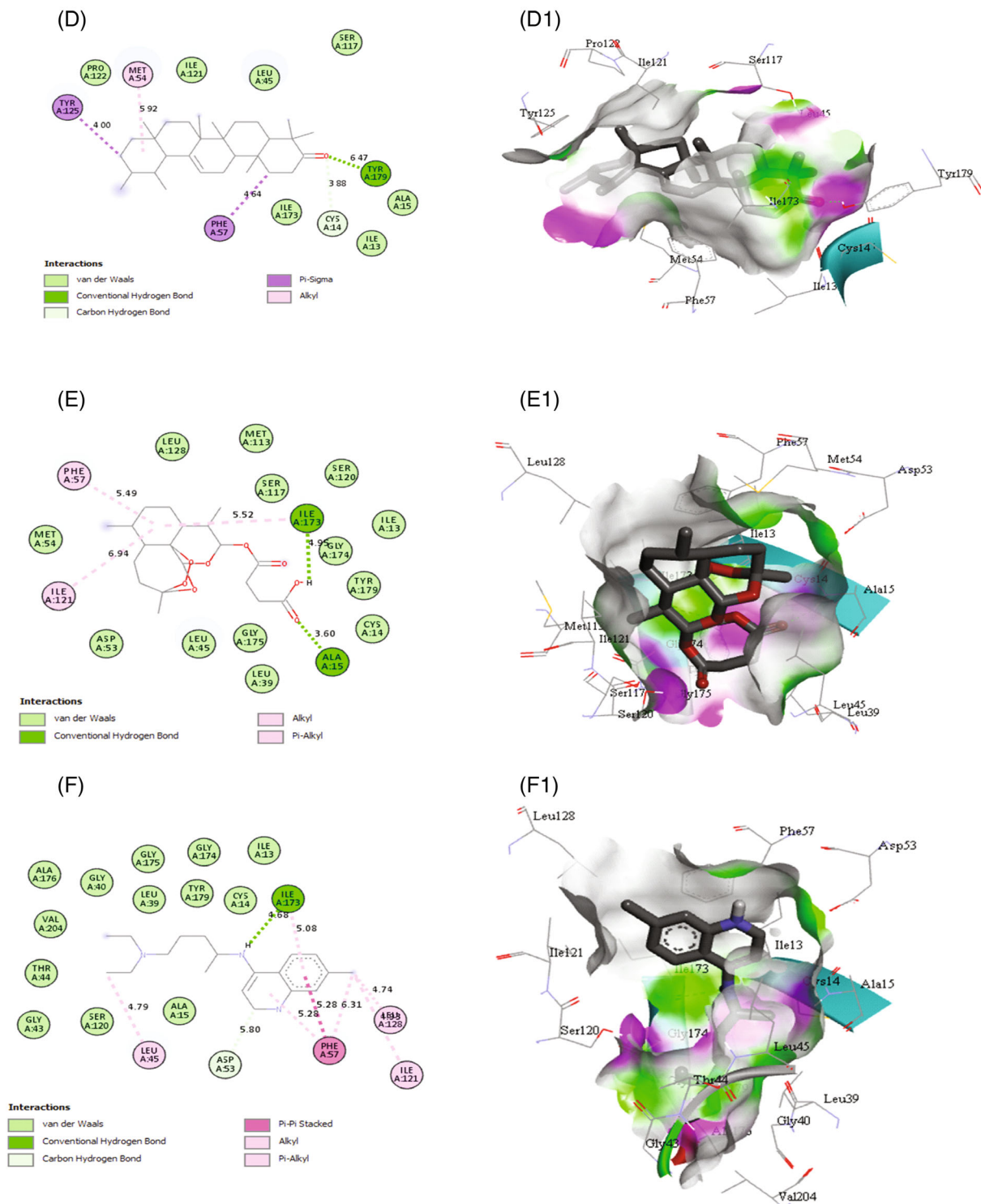


FIGURE 3 (Continued)

compounds have various levels of binding affinities for the *P. vivax* (2BL9) with Friedelin, Bauerenol, and epifriedelanol having  $-10.6$ ,  $-10.5$ , and  $10.3$  Kcal/mol binding scores, respectively (Table 5). Hence, Friedelin is the most potent inhibitor of 2BL9 when compared with the standard studied drugs (artesunate  $-9.4$  kcal/mol and chloroquine  $-7.1$  kcal/mol). The compounds Friedelin, Bauerenol, Epifriedelanol, Alpha-Amyrenone, Stigmasterol, and beta-Amyrin acetate interacted with 2BL9 as shown in Table 5. Important active site amino acid residues were in contact with the six compounds and the standard ligands like PHE A: 57 while Bauerenol and Stigmasterol, as well as the standard drugs, inhibited the catalytic activity of 2BL9 with alkyl and pi-alkyl hydrophobic interaction at the residue of an amino acid ILE A: 121, PHE A: 57, MET A: 54, LEU A: 128 and LEU A: 45. There were hydrophobic interactions with pi-sigma bonding with PHE A: 57 and TYR A: 125 and alkyl/pi-alkyl bonding with PHE A: 57, ILE A: 121 in all ligand-2BL9 complexes. Friedelin, Bauerenol, Epifriedelanol, Alpha-Amyrenone, Stigmasterol, and beta-Amyrin acetate could serve as lead molecular scaffolds for dihydrofolate reductase inhibitors.

### 3.8 | Molecular docking of ligands from A3 and standard drugs on target protein (4YCV)

From Table 6 and Figure 4B, the affinity of Cynaroside and 4YCV was highest ( $-10.5$  kcal/mol) within the binding pocket of Lysyl-tRNA synthetases (4YCV) at bond distances ranging from 3.17 to 7.17 Å dominated by hydrogen and carbon-hydrogen bonds. In context, the lowest affinity of the compound (Beta-Amyrin acetate) was stabilized at the binding energy of  $-9.9$  kcal/mol when compared with the artesunate ( $-8.1$  kcal/mol) and chloroquine ( $-5.6$  kcal/mol) in Table 6. The four compounds with the highest scores—Cynaroside, Quercimeritrin, Chrysoeriol, and Luteolin—that interacted with 4YCV to form complexes demonstrated that the compounds occupied the active sites (4A and 4B, respectively) of the enzyme. Three hydrogen bonds with cynaroside, quercimeritrin, luteolin, quercetin, and isorhamnetin

**TABLE 6** Ligands interaction with Lysyl-tRNA (ID 4YCV) synthetases and its amino acid residues.

S/No.	Compound CID	Name of compound	Molecular formula	Docking scores (kcal/mol)	Amino acid residues of 4YCV	Interactions	Bond length (Å)
1	5,280,637	Cynaroside	C <sub>21</sub> H <sub>20</sub> O <sub>11</sub>	-10.5	GLU A: 346	Pi anion	6.37
					GLU A: 500	2 Pi anion	5.89/7.17
					GLU A: 300	Unfavorable acceptor	4.37
					VAL A: 501	H-bond	5.40
					LEU A: 553	H-bond	5.57
					ARG A:559	H-bond	4.68
					ASN A: 339	Carbon H-bond	3.17
					ASP A: 558	Carbon H-bond	6.41
2	5,282,160	Quercimeritrin	C <sub>21</sub> H <sub>20</sub> O <sub>12</sub>	-10.3	THR A: 337	Carbon H-bond	6.27
					ASN A: 339	2 H-bond	3.02/4.72
					ARG A: 559	H-bond/pi-anion	6.65/5.31
					GLU A: 500	H-bond/pi-anion	5.45/6.58
					GLU A: 346	H-bond	4.43
					ASN A: 503	Carbon H-bond	4.47
					ARG A: 330	2 Pi anion	6.68/8.62
					PHE A:342	Pi-pi-stacked	4.76
GLU A300	Unfavorable acceptor	4.26					

(Continues)



TABLE 6 (Continued)

S/No.	Compound CID	Name of compound	Molecular formula	Docking scores (kcal/mol)	Amino acid residues of 4YCV	Interactions	Bond length (Å)
3	5,280,666	Chrysoeriol	C16H12O6	−10.0	ARG A: 559	H-bond/2 Pi-cation	3.69/5.26
					ASN A: 339	H-bond	4.37
					HIS A: 338	Pi-cation	5.22
					PHE A:342	2 Pi-pi-stacked	4.25/4.99
					GLU A: 346	Van der waal	5.25
4	5,280,445	Luteolin	C15H10O6	−9.9	VAL A: 501	H-bond	5.36
					THR A: 337	H-bond	5.34
					ASN A: 339	H-bond	4.29
					ARG A: 559	2 pi-cation	5.91/5.27
					HIS A: 338	Pi-cation	5.17
5	5,280,343	Quercetin	C15H10O7	−9.8	ARG A: 559	H-bond/2 pi-cation	3.76/5.33
					ASN A: 339	H-bond	4.34
					GLU A: 334	H-bond	4.56
					LEU A: 555	H-bond	4.63
					PHE A: 342	2 pi-stacked	4.27/4.99
					HIS A: 338	Pi-cation	5.17
					GLY A: 556	Carbon H-bond	3.49
6	5,281,654	Isorhamnetin	C16H12O7	−9.8	ARG A: 559	2 pi-cation	5.01/5.88
					VAL A: 501	H-bond	5.45
					ASN A: 339	H-bond	3.21
					GLU A: 332	H-bond	4.27
					HIS A: 338	Pi-cation	5.17
					PHE A: 342	2 pi-stacked	4.18/5.41
					GLU A: 346	Carbon H-bond	5.38
					GLY A: 556	Carbon H-bond	3.53
7	6,917,864	Artesunate	C19H28O8	−8.1	PHE A: 57	Pi-alkyl	5.49
					ILE A: 121	Alkyl	6.94
					ALA A: 15	H-bond	3.60
					ILE A:173	H-bond	4.90
8	2719	Chloroquine	C18H26ClN3	−5.6	ILE A:173	H-bond	4.68
					ILE A: 121	Alkyl	4.74
					PHE A: 57	Pi-pi-stacked	5.28
					LEU A: 45	Alkyl	4.79
					ASP A:53	Carbon-H	5.80

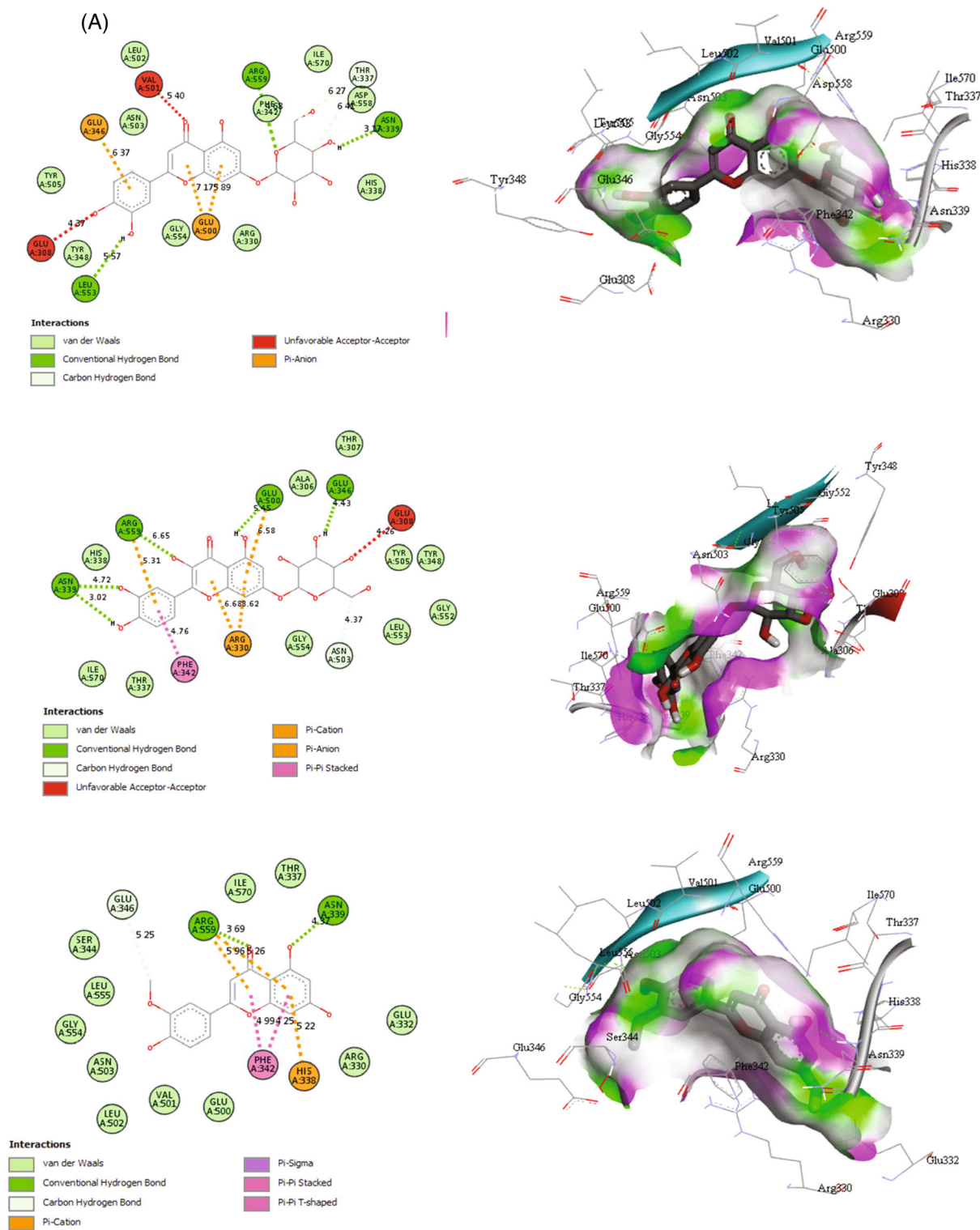


**FIGURE 4** 2D and 3D interaction of ligands and Amino acid residues of 4YCV. This shows the individual interactions and key amino acid residues for the inhibitor binding between 4YCV and (A): Cynaroside, (B): Quercimeritrin, and (C): Chrysoeriol. (A–C): 2D interactions, (A1–D1): 3D interactions. (D): Luteolin, (E): Artesunate, and (C): Chloroquine. (D–F): 2D interactions, (D1–F1): 3D interactions.

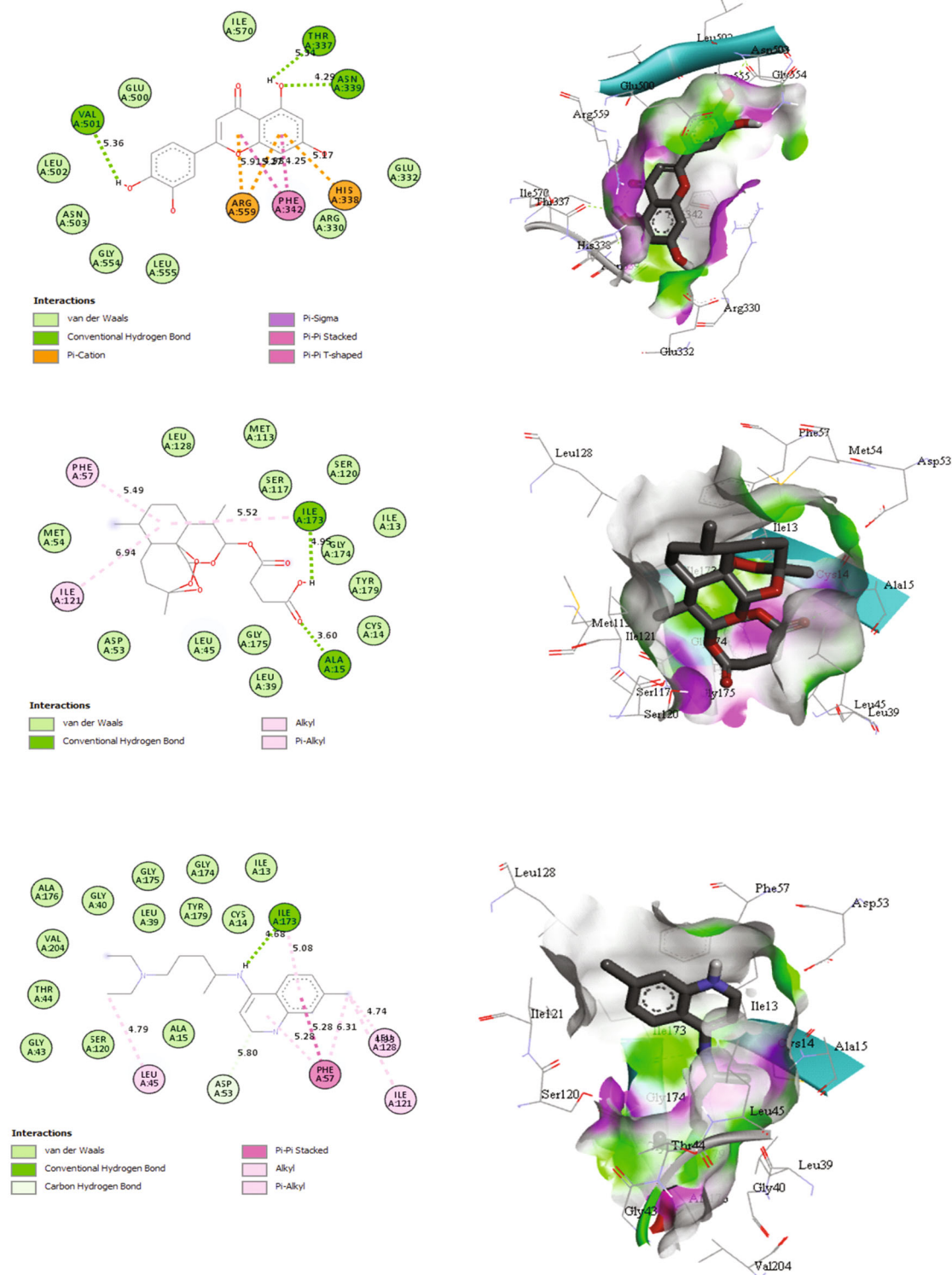


FIGURE 4 (Continued)

TABLE 7 Computational parameters of drug-likeness and ADME properties of compounds.

Compounds	MW (Da)	LOGP	HBD	HBA	nRB	TPSA (Å <sup>2</sup> )	Lipinski violation	Drug likeness	BioS	ESOL Log S	GIA
1	426.7	4.52	0	1	0	17.1	No	Yes	0.55	-8.66	Low
2	426.7	4.71	1	1	0	20.2	No	Yes	0.55	-8.16	Low
3	428.7	4.67	1	1	0	20.2	No	Yes	0.55	-8.85	Low
4	424.7	4.58	0	1	0	17.1	No	Yes	0.55	-7.95	Low
5	412.7	5.01	1	1	5	20.2	No	Yes	0.55	-7.46	Low
6	468.8	5.19	0	2	2	26.3	No	Yes	0.55	-8.74	Low
7	448.4	1.83	7	11	4	190.28	Yes	No	0.17	-3.65	Low
8	464.4	1.54	8	12	4	210.51	Yes	No	0.17	-3.04	Low
9	300.26	2.44	3	6	2	100.13	No	Yes	0.55	-4.06	High
10	286.24	1.86	4	6	1	111.13	No	Yes	0.55	-3.71	High
11	302.23	1.63	5	7	1	131.36	No	Yes	0.55	-3.16	High
12	316.26	2.35	4	7	2	120.36	No	Yes	0.55	-3.36	High

Note : Compounds 1 = Friedelin, 2 = Bauerenol, 3 = Epifriedelanol, 4 = Alpha-Amyrenone, 5 = Stigmasterol, 6 = beta-Amyrin acetate, 7 = Cynaroside, 8 = Quercimeritrin, 9 = Chrysoerio, 10 = Luteolin, 11 = Quercetin, 12 = Isorhamnetin, MW = molecular weight, HBD = hydrogen bond donor, HBA = hydrogen bond acceptor, nRB = no of rotatable bond, TPSA = total polar surface area, BioS, bioavailability score; Log Kp = skin permeation, GIA = Gastrointestinal absorption.

linked to the active site such as ARG A: 559, VAL A: 501, LEU A: 553, GLU A: 346, ASN A: 339, VAL A: 501, THR A: 337, GLU A: 334, ALA A: 15, ILE A:173, LEU A: 555 and GLU A: 332 and hydrophobic communications with LEU A: 45, PHE A: 57, HIS A: 338, PHE A: 342 and ARG A: 330 at the binding pockets of 4YCV. Two Carbon-H bonds with GLU A: 346, GLY A: 556, ARG A: 330, ASP A:53, and ASN A: 503 Van der Waal and Pi-cation interactions were additional interactions with ARG A: 330, ARG A: 559 and HIS A: 338. There was an unfavorable bond interaction between the ligand and GLU A: 300 residues of 4YCV. Unfavorable bonding has an impact on the drug's stability.

### 3.9 | Drug-likeness and pharmacokinetic breakdown

In this subsection, the ADME characteristics of the ligands were analyzed including the physicochemical properties, drug-likeness, and several other parameters using SwissADME. The results are shown in Table 7. The molecular weights of all the compounds fall below 500 DA with rotatable bonds within the range. Interestingly, gastrointestinal absorption showed that only compounds 9–12 have high GIA absorption; on the other hand, only compounds 7 and 8 violated Lipinski rule of five making the rest of the compounds good drug candidates.

## 4 | DISCUSSIONS

This section discussed the phytochemical composition of different extracts of *Artemisia annua*, specifically comparing fresh leaf extract (AF) and dry leaf extract (AD). As shown in Table 1, the Phytochemical concentrations in the aqueous dry (AD) extract of *Artemisia annua* ANAMED (A3) were significantly more ( $p < 0.05$ ) than those obtained from their fresh (AF) leaves extract. The results show that saponin content was significantly higher in AD compared to AF. Additionally, AD exhibited significantly higher values of flavonoids, alkaloids, and tannins compared to AF. The order of phytochemical concentrations in both AD and AF was found to be saponin > flavonoids > alkaloids > tannins. This could be accounted for by the fact that the AD extract is more concentrated than the AF extract since the latter has a moisture content that is often higher. The plant contains a significant group of polyphenols known as flavonoids. As a result of their ability to give hydrogen or electrons from the hydroxyl group on their phenolic ring, flavonoids and phenols play a crucial role as an antioxidant,<sup>33</sup> which explains why they are currently used as medicinal treatments for a variety of disorders.

The greatest class of secondary metabolites is alkaloids, which are mostly composed of nitrogen bases produced from amino acid building blocks and ammonia molecules.<sup>34</sup> The present study showed high mineral content of AD extract when compared with the AF counterpart, which could be explained by the higher moisture content of AF leaf extract. There was no trace of selenium either in AD or AF extracts (Table 2). It has been reported that Elemental selenium is insoluble in water and does not easily undergo reduction or oxidation in nature<sup>35</sup> relationship between iron deficiency and malaria incidence was observed by Benzecry et al.<sup>36</sup> Iron deficiency may be a sign of a lower socioeconomic position and a higher malaria risk as a result. According to Ekeh et al.<sup>37</sup> in areas where malaria is prevalent, iron and zinc deficiencies are usual and increase morbidity. The favorable effects of zinc on treating diarrhea may result from a direct impact of zinc on intestinal function due to enhanced water and electrolyte absorption.<sup>38</sup> Minerals are indispensable constituents of hormones, enzyme activation mechanisms, and biosynthesis of hemoglobin.<sup>39</sup>

Vitamins are organic molecules crucial in small amounts for metabolism and other healthy human growth. The outcome of this study revealed that the leaves *Artemisia annua* ANAMED is very much endowed with vitamin C which functions as an antioxidant and enzyme cofactor and function as a pro-oxidants scavenger and reduces oxidative stress; Vitamin E, in addition, regulates immunological response, inhibits lipid peroxidation.<sup>40</sup> Ekeh et al.<sup>37</sup> reported that zinc and vitamin C supplements help in the treatment of malaria because they increase PCV and HB, reduce mortality rates, and support the therapeutic effects of artemether.

Data on acute toxicity indicate that the extract did not result in any deaths in any of the doses. This was a clear sign that the doses utilized were safe. No physical or behavioral symptoms due to over-toxicity, such as diminished motor activity, and decreased body or limb tone, were noticed. This suggests that the extract's LD50 is higher than 5000 mg/Kg.

Since the 4-day suppressive test largely evaluates the antimalarial effectiveness of possible drug candidates on early infections, it is frequently used to screen for antimalarials. The most trustworthy metric is the calculation of the percent inhibition of parasitemia.<sup>41</sup> In typical screening trials, the test substance is usually considered to be active when the mean parasitemia is less than 90% relative to mock-treated control animals.<sup>42</sup> Both AD and AF extract significantly decreased the percentage parasitemia evaluated in the 4-day test in *Plasmodium berghei*-infected mice, as can be observed from the data; interestingly, AD extract was shown to have stronger blood schizontocidal activity than the AF, this could be since AD is more endowed with secondary metabolites as well as the minerals and vitamins which also possess antioxidant properties.

The endoperoxidation by sesquiterpenes and monoterpenes in secondary metabolites has been linked to antiplasmodial activity.<sup>43</sup> For example, the group of alkaloids includes quinine, one of the most reliable and conventional antimalarial treatments.<sup>44</sup> Alkaloids prevent the parasite from detoxifying heme into a safe malaria pigment.<sup>45</sup> This was demonstrated by the chemosuppression observed after the 4-day suppressive test (Figure 1), supporting the idea that the bioactive molecules in the AD may have been localized. The phytochemical components of the A3 may also work singly or in concert to exhibit their antimalarial activity. Nonetheless, the AF extract may contain traces of bioactive molecules compared to the AD extract, which could account for its decreased antimalarial efficacy. The fact that AF and AD extract of A3 enhanced the mean survival time of the experimental animals (not presented) suggests that the plant suppressed *P. berghei* and minimized the overall pathologic impact of the parasite on the mice. When compared to the untreated group, the higher dose (400 mg/kg) of AD and AF extract significantly decreased the percentage parasitaemia in the suppressive and curative tests. Also, it was noted that the treated groups had higher appetites than the control group; some bioactive substances may have appetite-stimulant effects that can boost hunger and metabolism in addition to parasite clearance. A decrease in parasitaemia percentage is directly related to the rise in percentage suppression tests. Because the haematopoietic system is the main target of hazardous substances, measures of hematological parameters are used to track the pathological and physiological conditions in both animals and humans.<sup>46</sup> Food and external objects are mostly transported by blood. Hemoglobin, platelets, RBCs, and WBCs are frequently exposed to larger dosages of harmful substances as a result, putting these parameters at risk. In comparison to the untreated group, most of the extracts significantly ( $p < 0.05$ ) raised PCV and RBC. Following ingestion of the extracts, a rise in red blood cells and its parameters suggest stimulation of healthy erythropoietic stem cells.

Similarly, there was a progressive decrease in the number of WBC in a dose-dependent way, this suggests a restorative potential of the extracts. Increased WBC (as observed in the untreated) also suggests that the extracts could possess immunological properties, which caused an enhanced proliferation of leucocytes for the protection of the body system. This suggests that the extracts could mount an immunological response in the case of external aggression. This agrees with the report of Dioka et al.,<sup>47</sup> who found that aqueous *Catharanthus roseus* leaf extract improved hematopoietic parameters in animal models. Differential leucocyte counts are signs of an organism's capacity to get rid of the infection. Seldom does an increase in circulating leukocytes reflect an increase in all leukocyte subtypes.<sup>48</sup> Therefore, increase in neutrophils in a



dose-dependent way suggests the ability of the extracts to stimulate neutrophil migration in response to chemoattraction. Such an increase could be a result of the existence of potent bioactive compounds in the AF and AD extracts that shielded leukocytes and thus affect the immune system and leukocyte differential counts<sup>49</sup>; to improve B- and T-cell differentiation and proliferation activities. The animals' phagocytic activity is improved by the higher neutrophil numbers.<sup>50</sup>

On the other hand, lymphocyte proliferation was manifest in 200 mg/kg b.w. of the extracts compared to their 400 mg/kg b.w counterparts. Notwithstanding, a notable rise ( $p < 0.05$ ) in lymphocyte count occurred in all the extract-treated groups when compared to the untreated. The decreased lymphocytes of the untreated groups could be due to oxidative stress activation orchestrated by malaria parasites, however, the increase in lymphocyte count of the treated groups might be due to lymphocyte migration a pathway toward resolution of inflammatory response and repair of tissue damage. The improvement in the lymphocyte counts in the present study may help boost the plasma/T cells of the immune system. This study agrees with the work of Adebayo et al.<sup>51</sup> which expressed that *Chrysophyllum albidum* improved leukocyte differential count. Similarly, increased levels of eosinophils suggest a prompt response to an increase in parasitaemia; during allergic reactions and parasitic infections, the number of eosinophils, multinucleated leukocytes with richly protein-filled granules, increases in the blood and at inflammatory sites.<sup>52</sup> It is thought that the protection against parasites mediated by eosinophils involves binding of the antigenic peptides by antibody or complement and then releasing intracellular granules which damage the invading parasites.<sup>53</sup> Eosinophil counts rise in response to parasitic infection.

All six compounds make close Pi-Sigma/alkyl/ Pi-pi-stacked connections with the amino residue(s) of 2BL9 (Figure 3A,B and Table 5). However, in each structure, the binding amino residue is rotated to allow for the best shape for the specific interactions. Nevertheless, it is possible that those hydrophobic interactions between PHE A: 57 and the aromatic ring of the compounds contributed to the binding scores. Thus, communications with PHE A: 57 are likely necessary for the 10 inhibitors' high-affinity binding. Hydrophobic interactions enhance a complex molecule's biological activity and aid in maintaining the biological surroundings of drug-target complexes.<sup>54</sup> This research identified crucial amino acid residues required for the binding of ligands to the residue of 2BL9, specifically, PHE A: 57 and ILE A: 121 which are vital for compound binding.<sup>55</sup> This enzyme's inhibition has been recognized as a key strategy for therapeutic malaria intervention.

Due to its application in finding novel protein ligands and its importance in structure-based drug design, molecular docking has had a substantial impact on the drug development process.<sup>56</sup> It is interesting to note that the ligands in this study with the highest docking scores interacted with these important residues at the Lysyl-tRNA synthetases' active site. Inhibition was measured by the binding energy.<sup>57,58</sup> The best docking and maximum affinity were achieved by the complex with lower binding energy.<sup>59</sup> *P. falciparum* and *P. vivax* must share common targets since future novel treatments must be effective against both parasites. *P. falciparum* and *P. vivax* protein targets must be conserved since future novel ant-malaria agents must be effective against both parasites. As shown in Figure 4 and sequentially, there are excellent interactions; some of the selected chemicals had conventional hydrogen and carbon-hydrogen bonds connected with them. The interactions between the —OH groups of the ligands: ARG A: 559 and ASN A: 339 are likely crucial for the high-affinity binding of the six inhibitors. The possibility of inhibitory action of these compounds may be attributed to the binding of the ligands with ARG A: 559 and ASN A: 339, which is an integral part of the enzyme active site and other amino acid residues required for catalytic activity. These interactions contribute to the binding energy. Unfavorable bonds in a receptor-ligand complex render it unstable since they are a sign that repelling forces are present. The strength and catalytic activity of a binding complex are anticipated by the hydrogen bonds connecting them.<sup>42</sup> Figure 3A,B depicts the amino acid residues with which hydrogen bonds were formed. All the selected compounds showed higher stability than Artesunate and chloroquine in their interactions with the Lysyl-tRNA synthetases (4YCV). This could account for the selected compounds' lower docking scores compared to artesunate and chloroquine. As a result, the target hit molecules exhibit competitive inhibition with artesunate and chloroquine and can be used as strong inhibitors of Lysyl-tRNA synthetases.

Undoubtedly, drug-likeness is an important factor to consider while screening antimalaria agents in the initial stages of drug development. This metric, namely its impact on the bioavailability when taken orally, can be thought of to match up the physicochemical properties of a substance with their biochemical properties in the body.<sup>60</sup> The stringent drug-likeness regulations (Lipinski's criteria: less than 10 HBA, a log P not larger than 5, an MW less than 500 g/mol, and less than 5 HBD) have been broken by cynaroside and quercimeritrin. The results of the ADME indicate that these compounds, except cynaroside and quercimeritrin, have a high oral bioavailability, where all the selected compounds have a computed value of 0.55 and can be absorbed in the intestine concerning the TPSA value of less than 140 Å<sup>2</sup> and the nRB value of less than 10, respectively<sup>61</sup>; hence fall within the category of drug-like substances. Interestingly, the rate and degree by which active moiety/ingredient is metabolized from a pharmaceutical product and then enter the bloodstream are referred to



as bioavailability<sup>57,58</sup> and therefore could reduce the risk of side effects and toxicity. Rats' bioavailability is thought to be influenced by the number of rotatable bonds (nRB), which has long been identified as a characteristic that is dependent on molecular flexibility.<sup>62</sup>

The ability of oral drugs to dissolve in an intestinal fluid is significant because poor solubility could prevent intestinal absorption through the portal vein system.<sup>63</sup> When the water solubility properties were examined (Table 7), Cynaroside, quercimeritrin, luteolin, quercetin, and Isorhamnetin were found to be soluble while predictably Friedelin, bauerenol, epifriedelanol, alpha-Amyrenone, stigmasterol, and beta-Amyrin acetate were poorly soluble. The distribution and absorption properties of a compound are greatly affected by its water solubility (log S).<sup>56</sup> There are two methods used to prewise water solubility using SwissADME: the first is the application of the Estimated SOLubility (ESOL) model (Solubility class: Log S Scale: Insoluble <−10, poorly <−6, moderately <−4, soluble <−2, very <0); the second is an adaptation of Ali et al.,<sup>64</sup> (Solubility class: Log S Scale: Insoluble <−10, poorly <−6, moderately <−4, soluble <−2, very <0). Interestingly, Friedelin, bauerenol, epifriedelanol, alpha-Amyrenone, stigmasterol, beta-Amyrin acetate, and Cynaroside were estimated to have low gastrointestinal absorption (GIA) while chrysoerio, luteolin, quercetin, and isorhamnetin have high gastrointestinal absorption, which is a highly favorable characteristic of a drug candidate, given the undeniable benefits of the oral route of administration. Several efforts have been made to accurately estimate GIA because it is thought to be one of the key factors that affect bioavailability.<sup>65</sup> The average values suggest that there is a good chance that the investigated bioactive compounds contain drug leads.

## 5 | CONCLUSION

This research has demonstrated the optimal method for preparing A3 tea for malaria treatment and highlighted its potential immunostimulatory effects. These findings provide valuable in silico validation for *Artemisia annua* as a promising target for antimalarial drug development. Consequently, these results suggest that it could serve as a potential therapeutic agent against Plasmodium. The study reveals that the phytochemicals present in *Artemisia annua* interact with specific amino acid residues, which are the primary targets for most *Plasmodium berghei* protease inhibitors. Furthermore, the biological activities observed are likely attributed to the presence of phytochemicals, vitamins, and minerals. It is recommended to conduct in vivo experiments to further validate these in silico findings. Future studies may also explore the application of machine learning algorithms for predictive analytics.

### AUTHOR CONTRIBUTIONS

**Kennedy Chinedu Okafor:** Project administration (equal); supervision (equal); writing – review and editing (equal). **Victor Onukwube Apeh:** Conceptualization (equal); writing – original draft (equal). **Ifeoma Felicia Chukwuma:** Conceptualization (equal); formal analysis (equal); investigation (equal); methodology (equal). **Henrietta Onyinye Uzoeto:** Conceptualization (equal); data curation (equal); investigation (equal); validation (equal). **Titus Ifeanyi Chinebuh:** Conceptualization (equal); formal analysis (equal); investigation (equal); methodology (equal); validation (equal). **Florence Nkechi Nworah:** Software (equal); validation (equal); writing – review and editing (equal). **Emmanuel Israel Edache:** Investigation (equal); methodology (equal); project administration (equal). **Okafor Ijeoma Peace:** Methodology (equal); resources (equal). **Okoronkwo Chukwunenye Anthony:** Project administration (equal); supervision (equal).

### ACKNOWLEDGMENTS

This work was supported by Nigeria Tertiary Education Fund under the grant number TETF/ES/UNIV/IMO STATE/TSAS/2021. We want to appreciate Rev Sister Rose Uke and her team (Nigeria) for supporting this research.

### CONFLICT OF INTEREST STATEMENT

The authors have no conflict of interest relevant to this article.


### PEER REVIEW

The peer review history for this article is available at <https://www.webofscience.com/api/gateway/wos/peer-review/10.1002/eng2.12831>.

## DATA AVAILABILITY STATEMENT

The current work created or examined data sets, which will be made available upon justifiable request.

## ORCID

Victor Onukwube Apeh  <https://orcid.org/0000-0003-2987-4046>  
 Kennedy Chinedu Okafor  <https://orcid.org/0000-0002-9243-6789>  
 Ifeoma Felicia Chukwuma  <https://orcid.org/0000-0002-8373-432X>  
 Henrietta Onyinye Uzoeto  <https://orcid.org/0000-0001-8897-1773>  
 Titus Ifeanyi Chinebu  <https://orcid.org/0000-0002-2143-7733>  
 Florence Nkechi Nworah  <https://orcid.org/0000-0002-7724-9846>  
 Okoronkwo Chukwunenye Anthony  <https://orcid.org/0000-0002-5098-9764>

## REFERENCES

- Patel RG, Singh A. Miniature medicine: Nanobiomaterials for therapeutic delivery and cell engineering applications. *IEEE Pulse*. 2014;5(2):40-43. doi:10.1109/MPUL.2013.2296801
- Haynes RK, Cheu KW, N'Da D, Coghi P, Monti D. Considerations on the mechanism of action of artemisinin antimalarials: part 1—the 'carbon radical' and 'heme' hypotheses. *Infect Disord Drug Targets*. 2013;13(4):217-277. doi:10.2174/1871526513666131129155708
- Müller J, Schlange C, Heller M, et al. Proteomic characterization of *Toxoplasma gondii* ME49 derived strains resistant to the artemisinin derivatives artemiside and artemisone implies potential mode of action independent of ROS formation. *Int J Parasitol Drugs Drug Resist*. 2023;21:1-12.
- Feng LU, Xin-Long HE, Richard C, Jun CA. A brief history of artemisinin: modes of action and mechanisms of resistance. *Chin J Nat Med*. 2019;17(5):331-336.
- Ménard D, Khim N, Beghain J, et al. Worldwide map of *Plasmodium falciparum* K13-propeller polymorphisms. *N Engl J Med*. 2016;374:2453-2464.
- Bhagat K, Kumar N, Kaur Gulati H, et al. Dihydrofolate reductase inhibitors: patent landscape and phases of clinical development (2001-2021). *Expert Opin Ther Patents*. 2022;32(10):1079-1095.
- Jaramillo Ponce JR, Théobald-Dietrich A, Bénas P, Paulus C, Sauter C, Frugier M. Solution X-ray scattering highlights discrepancies in Plasmodium multi-aminoacyl-tRNA synthetase complexes. *Protein Sci: Publ Protein Soc*. 2023;32(2):e4564.
- Ryutaro F, Shin-ichi Y, Riku S, et al. Amino acid specificity of ancestral aminoacyl-tRNA Synthetase prior to the last universal common ancestor Commonote commonote. *J Mol Evol*. 2022;90(1):73-94.
- Ayoola GA, Coker HA, Adesegun SA, et al. Phytochemical screening and antioxidant activities of some selected medicinal plants used for malaria therapy in southwestern Nigeria. *Trop J Pharm Res*. 2008;7:1019-1024.
- Efferth T, Kaina B. Toxicity of the antimalarial artemisinin and its derivatives. *Crit Rev Toxicol*. 2010;40(5):405-421.
- Haynes RK. From artemisinin to new artemisinin antimalarials: biosynthesis, extraction, old and new derivatives, stereochemistry and medicinal chemistry requirements. *Curr Top Med Chem*. 2006;509-537:509-537.
- Xiong Y, Huang J. Anti-malarial drug: the emerging role of artemisinin and its derivatives in liver disease treatment. *Chin Med*. 2021;16:80.
- WHO. World Malaria Report. 2021 <https://www.who.int/teams/global-malaria-programme/reports/worldmalaria-report-2020/>. Accessed 10 December 2021.
- Zhou Y, Gilmore K, Ramirez S, et al. In vitro efficacy of artemisinin-based treatments against SARS-CoV-2. *Sci Rep*. 2021;11:14571.
- Nair MS, Huang Y, Fidock DA, Towler MJ, Weathers PJ. *Artemisia annua* L. hot-water extracts show potent activity in vitro against Covid-19 variants including delta. *J Ethnopharmacol*. 2022;284:114797.
- du Preez-Bruwer I, Mumbengegwi DR, Louw S. In vitro antimalarial properties and chemical composition of *Diospyros chamaethamnus* extracts. *South Afr J Bot*. 2022;149:290-296.
- Abebe BM, Mestayet G, Eshetie MB, Desalegn AG. Antimalarial activity of seed extracts of *Schinus molle* against *Plasmodium berghei* in mice. *J Evid-Based Integr Med*. 2021;26:1-10.
- Chaniad P, Mathirut M, Apirak P, Parnpen V, Chuchard P. Antimalarial properties and molecular docking analysis of compounds from *Dioscorea bulbifera* L. as new antimalarial agent candidates. *BMC Complement Med Ther*. 2021;21:144.
- Vasquez M, Zuniga M, Rodriguez A. Oxidative stress and pathogenesis in malaria. *Front Cell Inf Microbiol*. 2021;11:768182. doi:10.3389/fcimb.2021.768182
- Nbaeyi-Nwaoha IE, Onwuka CP. Comparative evaluation of antimicrobial properties and phytochemical composition of *Artocarpus artilis* leaves in ethanol, n-hexane and water. *Afr J Microbiol Res*. 2014;8(37):3409-3421.
- Lorke A. A new approach to practical acute toxicity testing. *Arch Toxicol*. 1983;54(4):275-287. doi:10.1007/BF01234480
- Peter W, Portus H, Robinson L. The four day suppressive in vivo antimalarial test. *Ann Trop Med Para*. 1995;69:155-171.
- Kifle ZD, Adinew GM, Mengistie MG. Evaluation of antimalarial activity of methanolic root extract of *Myrica salicifolia* a rich (Myricaceae) against *Plasmodium berghei*-infected mice. *J Evid-Based Integr Med*. 2020;25:25.
- Ogbonna DN, Sokari TG, Agomuoh AA. Antimalarial activities of some selected traditional herbs from southeastern Nigeria against Plasmodium species. *Res J Parasitol*. 2008;3:25-31.

25. Anthonia O, Abosi, Raseroka BH. In vivo antimalarial activity of *Vernonia amygdalina*. *Br J Biomed Sci*. 2003;60:2:89-91. doi:[10.1080/09674845.2003.11783680](https://doi.org/10.1080/09674845.2003.11783680)
26. Apeh VO, Agu CV, Ogugua VN, et al. Effect of cooking on proximate, phytochemical constituents and hematological parameters of *Tetracarpidium conophorum* in male albino rats. *Eur J Med Plants*. 2014;4(12):1388-1399.
27. Ravindranath PA, Forli S, Goodsell DS, Olson AJ, Sanner MF. AutoDockFR: advances in protein-ligand docking with explicitly specified binding site flexibility. *PLoS Comput Biol*. 2015;11(12):e1004586. doi:[10.1371/journal.pcbi.1004586](https://doi.org/10.1371/journal.pcbi.1004586)
28. Potlitz F, Link A, Schulig L. Advances in the discovery of new chemotypes through ultra-large library docking. *Expert Opin Drug Discov*. 2023;18(3):303-313. doi:[10.1080/17460441.2023.2171984](https://doi.org/10.1080/17460441.2023.2171984)
29. Stewart JJ. Optimization of parameters for semiempirical methods VI: more modifications to the NDDO approximations and re-optimization of parameters. *J Mol Modell*. 2013;19:1-32.
30. Dallakyan S, Olson AJ. Small-molecule library screening by docking with PyRx. *Methods in Molecular Biology*. Vol 1263; Springer Nature; 2015:243-250.
31. Trott O, Olson AJ. AutoDockVina: improving the speed and accuracy of docking with a new scoring function, efficient optimization, and multithreading. *J Comput Chem*. 2010;31(2):455-461.
32. Lipinski CA, Lombardo F, Dominy BW, Feeney PJ. Experimental and computational approaches to estimate solubility and permeability in drug discovery and development settings. *Adv Drug Deliv Rev*. 2012;64:4-17.
33. Boadi NO, Badu M, Kortei NK, et al. Nutritional composition and antioxidant properties of three varieties of carrot (*Daucus carota*). *Sci Afr*. 2021;12:12.
34. Ugo NJ, Ade AR, Joy AT. Nutrient composition of Carica Papaya leaves extracts. *J Food Sci Nutr Res*. 2019;2:274-282.
35. Eszter BB, Shuxun S, Jiqian X, et al. Selenolanthionine is the major water-soluble selenium compound in the selenium tolerant plant *Cardamine violifolia*. *Biochim Biophys Acta (BBA) Gen Subj*. 2018;1862(11):2354-2362.
36. Benzecry SG, Alexandre MA, Vitor-Silva S, et al. Micronutrient deficiencies and *Plasmodium vivax* malaria among children in the Brazilian Amazon. *PLoS One*. 2016;11(3):e0151019. doi:[10.1371/journal.pone.0151019](https://doi.org/10.1371/journal.pone.0151019)
37. Ekeh FN, Ekechukwu NE, Chukwuma CF, et al. Mixed vitamin C and zinc diet supplements co-administered with artemether drug improved haematological profile and survival of mice infected with *Plasmodium berghei*. *Food Sci Hum Wellness*. 2019;8(3):12-22.
38. Roy SK, Behrens RH, Haider R, et al. Impact of zinc supplementation on intestinal permeability in Bangladeshi children with acute diarrhoea and persistent diarrhoea syndrome. *J Pediatr Gastroenterol Nutr*. 1992;15(3):289-296. doi:[10.1097/00005176-199210000-00010](https://doi.org/10.1097/00005176-199210000-00010)
39. Samson BO. Proximate and mineral composition of *Pentadiplandra brazzeana* stem bark. *Comput Appl Sci*. 2019;1:91-99.
40. Asensi-Fabado MA, Munné-Bosch S. Vitamins in plants: occurrence, biosynthesis and antioxidant function. *Trends Plant Sci*. 2010;15:582-592.
41. Bantie L, Assefa S, Teklehaimanot T, Engidawork E. In vivo antimalarial activity of the crude leaf extract and solvent fractions of *Croton macrostachyus* Hochst. (Euphorbiaceae) against *Plasmodium berghei* in mice. *BMC Complement Altern Med*. 2014;14:79. doi:[10.1186/1472-6882-14-79](https://doi.org/10.1186/1472-6882-14-79)
42. Biruk H, Sentayehu B, Alebachew Y, Tamiru W, Ejigu A, Assefa S. In vivo antimalarial activity of 80% methanol and aqueous bark extracts of *Terminalia brownii* Fresen. (Combretaceae) against *Plasmodium berghei* in mice. *Biochem Res Int*. 2020;2020:9749410. doi:[10.1155/2020/9749410](https://doi.org/10.1155/2020/9749410)
43. Hatzakis E, Opešenica I, Solaja BA, Stratakis M. Synthesis of novel polar derivatives of the antimalarial endoperoxides ascaridole and dihydroascaridole. *ARKIVOC*. 2007;8:124-135.
44. Mojarrab M, Shiravand A, Delazar A, Afshar HF. Evaluation of in vitro antimalarial activity of different extracts of *Artemisia aucheri* Boiss. and *A. Armeniaca* lam. and fractions of the most potent extracts. *Sci World J*. 2014;2014:825370.
45. Geremedhin G, Bisrat D, Asres K. Isolation, characterization and in vivo antimalarial evaluation of anthrones from the leaf latex of *Aloe percrassa* Todaro. *J Nat Remed*. 2014;14:119-125. doi:[10.18311/jnr/2014/72](https://doi.org/10.18311/jnr/2014/72)
46. Olson H, Betton G, Robinson D, et al. Concordance of toxicity of pharmaceuticals in humans and in animals. *Regul Toxicol Pharmacol*. 2010;32:56-67.
47. Dioka C, Orisakwe OE, Afonne J, et al. Investigation into the hematologic and hepatotoxic effects of Ribacin in rats. *J Health Sci*. 2012;48(5):393-398.
48. Maggini S, Wintergerst ES, Beveridge S, Hornig DH. Selected vitamins and trace elements support immune function by strengthening epithelial barriers and cellular and humoral immune responses. *Br J Nutr*. 2007;98(Suppl 1):S29-S35. doi:[10.1017/S0007114507832971](https://doi.org/10.1017/S0007114507832971)
49. Carr AC, Maggini S. Vitamin C and immune function. *Nutrients*. 2017;9(11):1211. doi:[10.3390/nu9111211](https://doi.org/10.3390/nu9111211)
50. Mishra N, Tandon VL. Haematological effects of aqueous extract of ornamental plants in male Swiss albino mice. *Vet World*. 2012;5:19-23.
51. Adebayo AJ, Abolaji AO, Opata TK, Adegbenro IK. Effects of ethanolic leaf extract of *Chrysophyllum albidum* G. On biochemical and haematological parameters of albino Wistar rats. *Afr J Biotechnol*. 2010;9(14):2145-2150.
52. Koubun Y, Etsushi K. Role of eosinophils in protective immunity against secondary nematode infections. *Immunol Med*. 2019;42(4):148-155.
53. Giacomini PR, Gordon DL, Botto M, et al. The role of complement in innate, adaptive and eosinophil-dependent immunity to the nematode *Nippostrongylus brasiliensis*. *Mol Immunol*. 2008;45(2):446-455.
54. Salo-Ahen OMH, Alanko I, Bhadane R, et al. Molecular dynamics simulations in drug discovery and pharmaceutical development. *Processes*. 2021;9(1):71.
55. Hayrettin OG, Muberra K. The hybrid compounds as multi-target ligands for the treatment of Alzheimer's disease: Considerations on donepezil. *Curr Top Med Chem*. 2022;22(5):395-407.

56. Bultum LE, Tolossa GB, Lee D. Combining empirical knowledge, in silico molecular docking and ADMET profiling to identify therapeutic phytochemicals from *Brucea antidysentrica* for acute myeloid leukemia. *PLoS One*. 2022;17(7):e0270050.
57. Apeh VO, Asogwa E, Chukwuma IF, Okonkwo OF, Nwora F, Uke R. Chemical analysis and in silico anticancer and anti-inflammatory potentials of bioactive compounds from *Moringaoleifera* seed oil. *Adv Trad Med*. 2022;22(1):59-74.
58. Apeh VO, Njoku OU, Nwodo OFC, Chukwuma IF, Abayomi EA. In silico drug-like properties prediction and in vivo antifungal potentials of *Citrullus lanatus* seed oil against *Candida albicans*. *Arab J Chem*. 2022;15(2):1-15.
59. Alamri MA, Alamri MA. Pharmacophore and docking-based sequential virtual screening for the identification of novel sigma 1 receptor ligands. *Bioinformatics*. 2019;15(8):586-595. doi:10.6026/97320630015586
60. Bickerton GR, Paolini GV, Besnard J, Muresan S, Hopkins AL. Quantifying the chemical beauty of drugs. *Nat Chem*. 2012;4(2):90-98.
61. Cheng F, Li W, Zhou Y, et al. Comprehensive source and free tool for assessment of chemical ADMET properties. *J Chem Info Model*. 2012;52(11):3099-3105.
62. Veber DF, Johnson SR, Cheng HY, Smith BR, Ward KW, Kopple KD. Molecular properties that influence the oral bioavailability of drug candidates. *J Med Chem*. 2002;45(12):2615-2623. doi: 10.1021/jm020017n.
63. Chukwuma IF, Nworah FN, Apeh VO, et al. Phytochemical characterization, functional nutrition, and anti-diabetic potentials of *Leptadenia hastata* (pers) Decne leaves: in Silico and in vitro studies. *Bioinf Biol Insights*. 2022;16:1-17.
64. Ali R, Chohan TA, Buabeid M, et al. Deep learning in drug discovery: a futuristic modality to materialize the large datasets for cheminformatics. *J Biomol Struct Dyn*. 2023;41(18):9177-9192. doi:10.1080/07391102.2022.2136244
65. Yan A, Wang Z, Cai Z. Prediction of human intestinal absorption by GA feature selection and support vector machine regression. *Int J Mol Sci*. 2008;9(10):1961-1976.

**How to cite this article:** Apeh VO, Okafor KC, Chukwuma IF, et al. Exploring the potential of aqueous extracts of *Artemisia annua* ANAMED (A3) for developing new anti-malarial agents: In vivo and silico computational approach. *Engineering Reports*. 2024;6(9):e12831. doi: 10.1002/eng2.12831